

## Review



**Cite this article:** Maclennan J. 2019 Mafic tiers and transient mushes: evidence from Iceland. *Phil. Trans. R. Soc. A* **377**: 20180021. <http://dx.doi.org/10.1098/rsta.2018.0021>

Accepted: 16 October 2018

One contribution of 15 to a Theo Murphy meeting issue ‘Magma reservoir architecture and dynamics’.

### Subject Areas:

volcanology, petrology, geochemistry, geophysics, geology

### Keywords:

iceland, petrology, volcano

### Author for correspondence:

J. Maclennan

e-mail: [jcm1004@cam.ac.uk](mailto:jcm1004@cam.ac.uk)

# Mafic tiers and transient mushes: evidence from Iceland

J. Maclennan

Department of Earth Sciences, University of Cambridge, Cambridge, UK

 JM, 0000-0001-6857-9600

It is well established that magmatism is trans-crustal, with melt storage and processing occurring over a range of depths. Development of this conceptual model was based on observations of the products of magmatism at spreading ridges, including Iceland. Petrological barometry and tracking of the solidification process has been used to show that the Icelandic crust is built by crystallization over a range of depths. The available petrological evidence indicates that most of the active rift zones are not underlain by extensive and pervasive crystal mush. Instead, the microanalytical observations from Iceland are consistent with a model where magmatic processing in the lower crust occurs in sills of decimetric vertical thickness. This stacked sills mode of crustal accretion corresponds to that proposed for the oceanic crust on the basis of ophiolite studies. A key feature of these models is that the country rock for the sills is hot but subsolidus. This condition can be met if the porosity in thin crystal mushes at the margins of the sills is occluded by primitive phases, a contention that is consistent with observations from cumulate nodules in Icelandic basalts. The conditions required for the stabilization of trans-crustal mushes may not be present in magmatic systems at spreading ridges.

This article is part of the Theo Murphy meeting issue ‘Magma reservoir architecture and dynamics’.

## 1. Introduction

It is well established that terrestrial magmatism is predominantly *trans-crustal*, meaning that magma batches are thought to be processed over a range of depths within the crust and uppermost mantle [1]. Of particular relevance for this contribution is that the trans-crustal

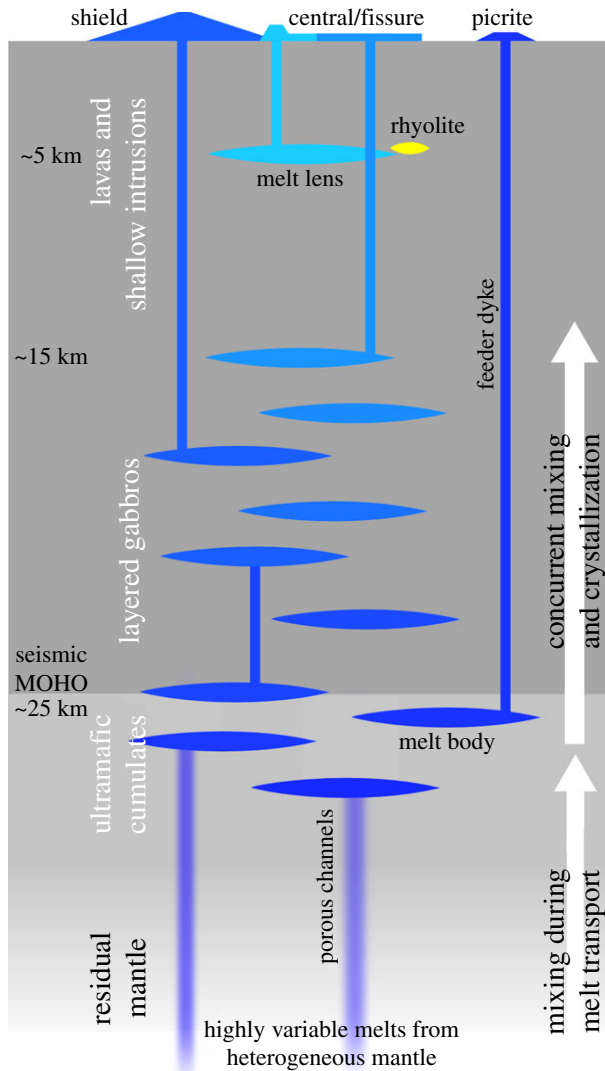


**Figure 1.** Schematic image of a model of magma storage and transport under an Icelandic rift-zone volcanic system, adapted from [2,3]. The observations and interpretations used to develop this model are described in the main text. Storage, cooling and crystallization are trans-crustal. Magma storage is dominated by stacked sills which may have a vertical thickness of about 10 m. Some eruptions are fed directly and rapidly from near-Moho magma storage zones, and undergo minimal interaction with the crust in transit. Pervasive, trans-crustal mush is not a feature of this model. Transient, spatially restricted mush zones are, however, present around the open liquid of the thin sills. (Online version in colour.)

nature of magma storage and crustal accretion has been the consensus view of Icelandic magmatism (figure 1) for almost 20 years [2,4].

Simplistic textbook models of volcanic systems involve the supply of eruptions from a single, shallow magma chamber which is itself fed directly from the mantle. Icelandic volcanic systems (figure 2) do not conform to this model and provide strong evidence for the storage of melts at a range of depths in the crust. Furthermore, figure 1 shows that eruptions can be fed directly from storage zones as deep as the Moho (20–40 km under Iceland) or from as shallow as 5 km. Global observations from geology, geophysics and petrology have been used to argue for *stacked-sills* or

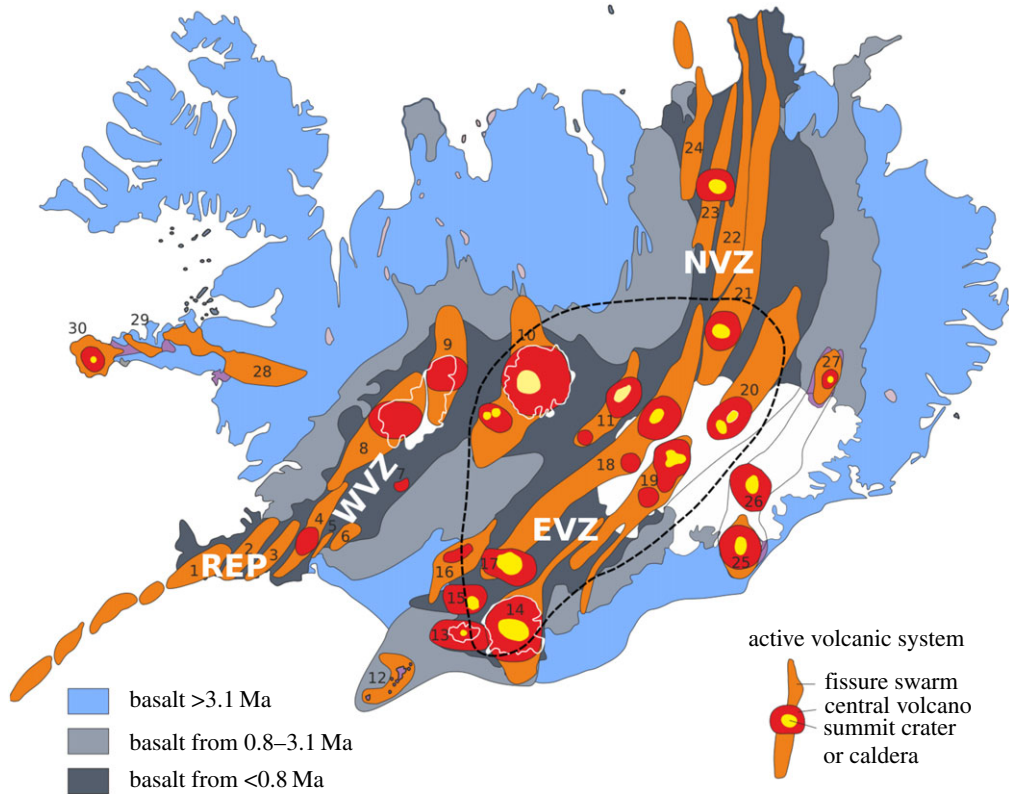


**Figure 2.** Map of the volcanic systems of Iceland, adapted from [5,6]. The volcanic systems are numbered. The active rift zones sit within the bands of relatively young basalt (<0.8 Ma) and are labelled: NVZ—Northern Volcanic Zone; EVZ—Eastern Volcanic Zone; WVZ—Western Volcanic Zone; REP—Reykjanes Peninsula. Most of the work described in this paper is based on a study of the Krafla and Theistareykir volcanic systems, numbered 23 and 24 respectively. The dashed line is based on [7] and encircles the rift zone volcanoes that sit on crust that is >35 km thick. The crust under the Reykjanes Peninsula (systems 1–3) and Krafla/Theistareykir is about 20 km thick. This study focuses on the active rift zones of the NVZ, WVZ and REP outwith the dashed line. (Online version in colour.)

*trans-crustal* models. Magma must be stored for sufficient duration at a given depth to leave a recognizable imprint of storage on these observational records.

Geophysical imaging of seismic velocity structure or resistivity provides a snap-shot of a magmatic system at the present day, but with limited spatial resolution and poor accuracy in the recovery of desirable properties such as temperature and porosity. Ancient plutonic bodies can be studied at high spatial resolution, from micrometres to kilometres [8]. Plutonic rocks, however, may be influenced by magmatic and near-solidus processes operating over a wide range of time scales ( $10^3$ – $10^{12}$  s). It can therefore be challenging to make the link between geophysical images of active magmatic systems that capture one moment in time and petrological observations of solidified plutonic rocks that record a temporally integrated signal. For example, does petrological evidence of late-stage fluid flow at low porosity from plutonic rocks have significance for the seismic observations, or the overall fluxes of mass and heat in the magmatic system?

The petrology of volcanic rocks provides some complementary information about a magmatic system that may be helpful in linking the plutonic record to geophysical observations. Erupted liquid compositions record conditions of final equilibration and perhaps the depth of storage [9–12]. The cargo of crystals and nodules carried to the surface with these liquids provides another opportunity to determine the depths of magma crystallization and storage [13,14]. Such petrological barometry has been a key part of establishing the importance of multi-tiered

magmatic processing beneath individual volcanic systems. Some of the crystal cargo appears to have escaped the protracted overprinting which complicates the interpretation of plutonic rocks. These volcanic samples can therefore provide a clearer record of the time scales of processes operating in the magmatic system. The rapid development of diffusion chronometry is helping to sharpen these temporal controls [15–17]. In certain cases, nodules of disaggregating magmatic mushes are brought to the surface, which can be used to investigate processes taking place at the margins of the open liquid of a magma chamber [18,19].

In a handful of systems, where recent eruptions have taken place and geophysical monitoring is available, it has been possible to directly link the petrological barometry to depths of magma storage inferred from seismic or geodetic data [20,21]. While this barometry may provide some spatial control on the depth of crystallization and magma storage, it is extremely challenging to use the crystal cargo of volcanic eruptions to infer anything about the spatial arrangement of the components of that cargo on a scale of  $<10^3$  m within the storage zones. Furthermore, the volumes of individual eruptions are typically a tiny fraction of that of the magmatic system and these eruptions can only sample parts of the system where the magma is mobile. The utility of volcanic petrology is greatly enhanced when it can be combined with geophysical constraints on the crustal structure or magma movement. It is important and alluring to make the link between petrological and geophysical data. This connection is, however, seldom straightforward. Misrepresentation and misunderstanding of the different data types can lead to erroneous models of sub-volcanic structure.

The purpose of this manuscript is to assess modern conceptual models of trans-crustal magmatism using the substantial body of detailed petrological observations available from Iceland's active volcanic regions.

## 2. Trans-crustal mush or solid country rock?

The building consensus regarding the trans-crustal nature of magma storage has been mirrored by an increasing incidence of conceptual models of active magmatic crust that involve large quantities of mush (figure 3). Mush is normally used to refer to mechanical mixtures of melt and crystals with interconnected solid and liquid. As porosity increases crystals disaggregate and the mixture can be referred to as magma: interconnected liquid without interconnected solids. In some conceptual models the crust has developed into a large pile of mush, with separated pockets of transient, higher porosity magma chambers [1,25]. Not all models of multi-tiered magmatism involve pervasive mush: the influential *stacked-sills* models of oceanic crustal accretion are built upon sills of  $\sim 10$  m height that are separated by hot, but subsolidus, cumulate rock [22,26–28]. These sills are likely to have thin mushy layers on their margins. In both conceptual models, mush-dominated and rock-dominated, the final products of magmatism have transitioned from mush to rock. The key difference is the proportion of the crust that is mushy at any one time and, accordingly, the duration of the transition from mush to rock.

Unfortunately, geophysical imaging seldom provides sufficient spatial resolution to be able to distinguish between pervasive mush and stacked sills [1,29]. The typical wavelengths of seismic energy that can be used to investigate magmatic systems preclude imaging of individual features of less than a few hundred metres extent. When low velocity zones or high  $V_p/V_s$  regions are imaged, the standard interpretation is that these indicate regions of higher melt fraction over the lengthscales of hundreds of metres. The effective properties of this block of rock might be the result of increased porosity in a uniform mush with melt evenly distributed at the crystal scale ( $10^{-3}$ – $10^{-2}$  m). Alternatively, these regions may correspond to volumes of solid rock that contain a higher proportion of melt pockets on a greater length-scale ( $10^1$ – $10^2$  m): decimetric sills in hot, subsolidus country rock.

Reflection seismic data collected above submarine volcanoes, most notably at spreading ridges, has a higher frequency content and can be used to image smaller features. The axial melt lens has been imaged as a strong reflector beneath some segments of the mid-oceanic ridge system [30–33]. In one case on the southern East Pacific Rise, full waveform inversion modelling

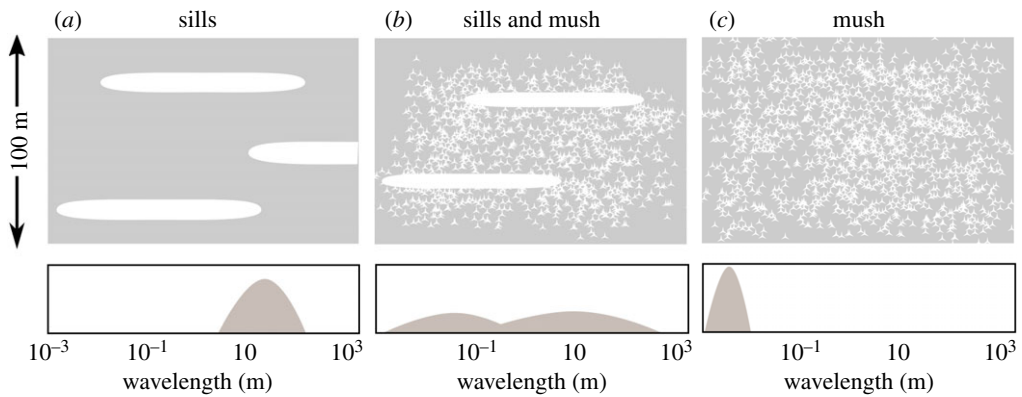


**Figure 3.** Possible distributions of melt in the porosity structure of a 100 m scale block of lower crust in an active volcanic system. (a) An end-member model, where the melt is stored in sills of decimetric thickness and surrounded by solid country rock. This model is close to that suggested by [22] for ophiolites and fast-spreading ridges in general and [2,3] for Iceland. The lower panel shows an example power-spectrum of the porosity distribution for this case. (b) A mixed model where melt pockets can be created within a pervasive mush, similar to the model presented by [1]. (c) Pervasive, evenly distributed mush, with most of the power in the porosity distribution concentrated at millimetric scales. The lower crust of mid-ocean ridge volcanic systems has previously been viewed as such a mush [23,24]. (Online version in colour.)

was used to argue for the presence a 50 m thick axial melt lens, with a solid roof and floor [31]. In another, at the Juan de Fuca Ridge, a near-ridge lower crustal melt lens of  $\sim 100$  m thickness was reported but it was not clear whether the host material for the melt was mush or solid rock [32]. These studies indicate that melt-rich sills on the decimetric scale do exist in magmatic systems, but they do not exclude a role for a pervasive mush pile in these same systems.

### 3. Mid-ocean ridges: stacked sills in mostly solid rock?

Mid-ocean ridge systems provide an excellent opportunity for understanding magmatic processes more generally. There are several good reasons to look carefully at spreading systems as a complement to arcs. A crucial advantage is that the tectonic setting allows for accurate reconstruction of the long-term flux of mass and heat through the system because for most mid-ocean ridges we know the spreading rate and for many segments an estimate of the crustal thickness is available. These features have aided the development of thermal models of mid-ocean ridge accretion with the incorporation of mechanical or petrological details to match observations from ridges and ophiolites [34–37]. Conceptual models of magmatism at mid-ocean ridges have evolved from the multi-kilometre-scaled, Stillwater-inspired models of axial vats of liquid [38] through to models with much more modest porosities. Many models now involve the presence of a small axial melt lens of limited vertical extent ( $< 200$  m). Over the decades, key arguments have focused on whether this axial melt lens is the principal source of solid cumulate material that makes up the lower crust (the *gabbro glacier* [35,39,40]) or the shallowest of a vertical stack of thin sills beneath the axis (the *stacked sills* model [22,26–28]). Consensus is now building around a hybrid model of accretion, hinted at by [22] and found to be consistent with thermal models and geophysical, petrological and geological observations from active ridges and ophiolites [36] and cooling rate constraints [41].

Some conceptual models of mid-ocean ridges have involved substantial quantities of mush between the shallow axial melt lens and the Moho [23,24]. If the intergranular liquid is widely distributed then this can have significant consequences for the mechanical properties of the lower crust and the plausibility of the lower-crustal flow required in gabbro-glacier models. Korenaga and Kelemen [26,27] carried out a detailed examination of rock and mineral compositional

zonation in cumulate gabbros from close to the Moho that are exposed in the Oman ophiolite. First, they concluded that the cumulate rocks had formed in small, open-system, melt-filled lenses near the Moho [26]. Next, they used correlations in mineral compositions (e.g. Ni and Mn in olivine cores preserved over the lengthscales of the sills) to argue that melt flux through the mush could account for less than 1% of the total melt flux for the ridge system [27]. In this model, the dominant mode of melt transport would be through high porosity, possibly open, vertical channels. The absence of important flux through the intercrystalline space indicates that pervasive interconnected porosity was not available. Their model of lower-crustal accretion involves decimetric sills encased in near-solidus rock.

More recently, Lissenberg & MacLeod [42] have reported abundant evidence at the crystal and hand-specimen scale for reactive porous flow in cumulate rocks from the lower oceanic crust. These rocks must have been part of a mush that was open to chemical exchange during the occlusion of porosity. The question remains, however, about how these observations of trace element zonation in clinopyroxene can be related to a quantification of the intercrystalline melt flux, and the temporal and spatial persistence of pervasive mush in the oceanic lower crust.

#### 4. Iceland: a volcanic window into oceanic crustal accretion

The presence of a mantle plume under the Mid-Atlantic Ridge generates oceanic crust of 20–40 km thickness at Iceland [7]. Active volcanism takes place on approximately 30 volcanic systems, which are grouped into a number of volcanic zones (figure 2). These zones are either classified as flank zones or rift zones. The flank zones, including systems 25–30 in figure 2, host alkaline magmatism and do not accommodate a substantial portion of the plate spreading. By contrast, the rift zones generate tholeiitic magma and accommodate the bulk of the extension associated with the full spreading rate of  $20 \text{ mm yr}^{-1}$ . The two northernmost volcanic zones of the Northern Volcanic Zone (NVZ) are Theistareykir (system 24) and Krafla (system 23). These systems have been the focus of detailed petrological work by groups from Cambridge and the University of Iceland—much of which is described below. The petrology, geochemistry and volcanic structure of other systems in the NVZ and those of the Western Volcanic Zone (WVZ) and Reykjanes Peninsula (REP) have also been the target of study [43–46]. The available observations indicate that models of crustal magmatic plumbing for these systems (1–4, 8, 21, 22 from figure 2) have much in common with Krafla and Theistareykir. This similarity may reflect the fact that the crustal thicknesses and magmatic fluxes in these systems are equivalent. It may also be important that these volcanic zones have been active for more than 5 Myr. By contrast, activity on the Eastern Volcanic Zone (EVZ: systems 12–20) started relatively recently (3 Ma). This region of high magma flux hosts volcanic systems that are petrologically and volcanically distinct from the rest of Iceland's rift zones. For example, the EVZ volcanic output is characterized by giant fissure eruptions and explosive eruptions from large central volcanoes, while the NVZ and WVZ contain large lava shields and monogenetic subglacial tuyas [47]. These observations indicate that models of magma transport and storage that are applicable to the EVZ are not entirely appropriate for the NVZ, WVZ and REP. This contribution therefore focusses on observations and models for Krafla, Theistareykir and the broader NVZ, WVZ and REP.

##### (a) Barometry indicates stacked-sills accretion

It has proven difficult to use the erupted products of mid-ocean ridge volcanoes to test models of magmatic systems because the  $1\sigma$  pressure uncertainties in many petrological barometers of  $\pm 1.5 \text{ kbar}$  are equivalent to a depth of  $\pm 4.5 \text{ km}$ , greater than the thickness of typical oceanic crust [9–14]. However, Iceland's thick crust allows petrological barometry to be used to establish whether eruptions are fed from storage zones at different depths as might be expected from a *stacked-sills* accretion model, or if they are all fed from a single shallow storage zone, consistent with *gabbro-glacier* style accretion. A study of the Krafla and Theistareykir volcanic systems in the NVZ (figure 2) used petrological barometry to show that magmas stored at a range of

depths in the crust and uppermost mantle (5–30 km) can be fed to the surface for eruption [2]. This barometry was based on both clinopyroxene-liquid equilibrium (see [14] for the most up-to-date iteration of this method) and parameterization of the composition of liquids that are in equilibrium with olivine, plagioclase and clinopyroxene as a function of pressure [10,21].

These barometers have undergone substantial improvement over the last 15 years, but the original conclusion is robust. Furthermore, the relationship between the estimated depth of equilibration and the extent of crystallization indicates that solid material is being added uniformly throughout the lower and middle crust under the NVZ [3]. These findings are consistent with a *stacked-sills* model of accretion (figure 1), which is significant because seismic imaging indicates that the Krafla volcanic system hosts a shallow melt lens [48] and therefore this imaged lens is simply the shallowest of a number of storage zones within the crust of the NVZ.

## (b) Macrocrysts, melt inclusions, carrier liquids and mush

These barometric findings not only show that Icelandic magmatism is trans-crustal: they also have significance for understanding the distribution of mushy zones within the Icelandic crust. This significance is most easily understood when the barometric results are combined with the findings of detailed microanalytical studies of the crystal cargoes of Icelandic mafic eruptions [43]. These eruptions often carry macrocrysts of olivine, plagioclase, clinopyroxene and more primitive magmas sometimes contain chromian spinel. Clean matrix glasses, available in tephra or as pillow-rims, provide a reliable estimate of the composition of the liquid that carried the crystals to the surface for eruption. Large glassy melt inclusions are present in these macrocrysts, and several hundred of these have been analysed for their trace element content by ion-microprobe.

The rims of the macrocrysts are almost always in equilibrium with the carrier liquid as far as a chemical exchange (e.g.  $K_d^{\text{Fe-Mg}}$  for olivine) or textural criteria are concerned. The macrocryst cores, however, are almost always too primitive (high in Mg# or An content) to be in equilibrium with the carrier liquid [43,49].

The relationship between the trace element composition of the melt inclusions and those of the carrier liquid is also systematic. Trace element ratios such as La/Yb, which are little affected by crustal processes in Iceland, show enormous diversity in olivine-hosted melt inclusions. This diversity has its origins in the fractional melting of compositionally heterogeneous mantle [50]. Inter-eruption variation in a carrier liquid compositions from single volcanic systems is substantial (e.g. La/Yb varies from 0.4 to 4.0 in Theistareykir primitive lava flows over the last 30 kyr), but intra-flow variation in carrier liquids in Icelandic basaltic eruptions is muted [43,51]. However, melt inclusions from single eruptions can show diversity in certain chemical indicators of mantle melt heterogeneity that is greater than the full diversity available in rock samples from a single volcanic system [43]. The crucial point here is that the average La/Yb of melt inclusions from a single eruption is very similar to that of the carrier liquid for that eruption [43]. Furthermore, in any given eruption, the variance of melt inclusion compositions drops as a function of the forsterite content of the host olivine. The inclusions within the least forsteritic macrocrysts, the macrocrysts closest to major-element equilibrium with the carrier, also have limited trace element variability.

These observations are summarized in figure 4 and strongly suggest that the macrocrysts have a well-defined relationship with the liquid that carries them to the surface. They are not xenocrysts picked up from cumulate rock or mush that was encountered on the transit path as the carrier liquid ascended prior to eruption. It is instead likely that these macrocrysts were derived by disaggregation of a crystal mush that formed on the walls of the magma body where storage and evolution of the carrier liquid took place. The mushy regions may form thin fringes round the sills of open liquid, rather than pervasive trans-crustal mushes.

The observations can be accounted for by a model where diverse mantle melts enter a storage region at depth, undergo concurrent mixing, cooling and crystallization to produce a

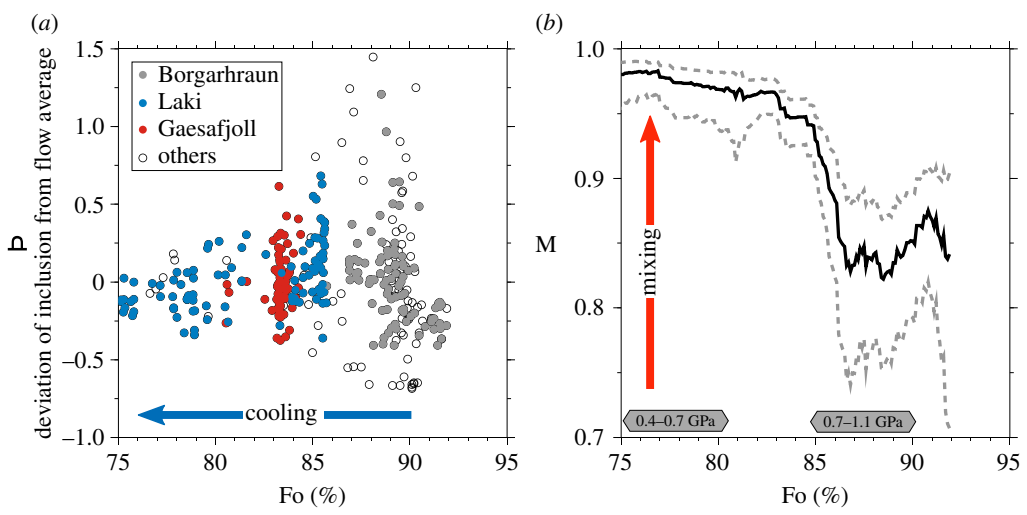


**Figure 4.** (a) Diversity of melt inclusion trace element composition plotted as a function of the composition of the olivine host (Fo%). Plot adapted from [43] with data from Laki [52]. The data are aggregated from 10 eruptions, and the general pattern of reduced variability at lower host forsterite content is recapitulated within the products of individual eruptions, most notably Borgarhraun. The mean deviation is close to zero, highlighting the strong and systematic relationship between the trace element composition of the olivine-hosted melt inclusions from a given eruption and the composition of the carrier liquid. (b) Variation in the mixing parameter,  $M$ , quantifying the mixing process. The grey boxes show the results of petrological barometry for different eruptions. Vigorous mixing of compositional heterogeneity in mantle melts takes place in the lower crust. (Online version in colour.)

relatively evolved and homogeneous melt. This melt then carries some of the disaggregated mushy products of this interval of cooling and crystallization upwards for eruption.

These observations indicate that magma can rise from close to the Moho and reach the surface without entraining observable quantities of crystal cargo *en route*. This magma is unlikely to have encountered mushy regions on its trans-crustal path, indicating that even in volcanic areas of relatively high magma flux such as Iceland, the crust remains dominantly solid. This point is neatly exemplified by pairs of eruptions which took place within a few thousand years of each other, have vents within a few kilometres of each other, but yet have compositionally distinct cargoes of olivine macrocrysts and melt inclusions. Good examples are Bóndhólshraun and Gaesafjöll in the Theistareykir volcanic system (number 24, figure 2) and Stapafell and Háleyjabunga in the Reykjanes system (number 1, figure 2). For each of these flows, the melt inclusion mean trace element composition is equivalent to that of the carrier liquid [43].

The strong relationship between carrier liquid and crystal cargo for individual eruptions and the clear difference in carrier liquid and crystal cargo between eruptions indicates that eruptions that are closely related in time and space may have separate plumbing systems. If melts had to transit a pervasive trans-crustal mush prior to eruption it is likely that their crystal cargoes would show less well-defined relationships with the carrier liquid (e.g. melt inclusion trace element mean would not be equal to that of the melt) and the crystal cargoes of separate eruptions would show significant overlap in their compositional range. The balance of petrological evidence from the NVZ, WVZ and REP of Iceland therefore indicates that pervasive trans-crustal mushes are not present under the main active rift zones [43].

Recent work using diffusion chronometry has established that these carrier liquids and their crystal cargoes rise from near-Moho depths of ~20 km and reach the surface in as little as 4 days in the case of the Borgarhraun eruption in the Theistareykir system [53]. It is difficult to envisage how these ascent rates, and the preservation of high equilibrium pressures in both OPAM and clinopyroxene-liquid barometers, can be reconciled with passage through a crust that contains a pervasive crystal mush.



## 5. Creating solid rocks in the lower crust

The previous sections have summarized some of the arguments for trans-crustal magmatism in oceanic-ridge settings and particularly in Iceland. In well-studied cases it is clear that melt and crystal cargoes can ascend rapidly from the Moho to the surface and preserve no evidence for interaction with pervasive trans-crustal mush. One such well-studied eruption is Borgarhraun, an 8000 year old primitive basalt/picrite flow from the Theistareykir volcanic system. The available petrological evidence from the active rift zones of the NVZ, WVZ and Reykjanes Peninsula indicates that the bulk of the crystal cargo is derived from mush that is closely related to the carrier liquid—perhaps from thin mushy layers at the margins of small melt-dominated sills. If the crust under these active volcanic zones is not mushy, it is worth understanding what processes might lead to the generation of solid country rock for the magma bodies that build the crust by crystallization.

Observations of the mineralogy of cumulate nodules brought to the surface by primitive eruptions such as Borgarhraun indicates that cumulate wehrlites and gabbros are present in the country rock of the near-Moho storage zones. The nodules contain phases that formed at high pressures and temperatures, with major and trace element compositions in equilibrium with liquids that could plausibly have mixed to form the Borgarhraun carrier liquid [54,55]. For example, in the wehrlitic nodules, highly forsteritic olivine chadacrysts are encapsulated in high Mg# clinopyroxene oikocrysts. Both the primocrysts and the interstitial crystals were in equilibrium with primitive liquids: no evidence is preserved of differentiated liquids produced by *in situ* crystallization. Chemical exchange between the interstitial liquids and the primitive melt in the chamber must have been effective.

The cooling interval preserved in the range of olivine core compositions present in the Borgarhraun products is  $\sim 100^{\circ}\text{C}$ . Therefore, hot, near-primary, melts stall in a storage zone and cool and crystallize, losing heat to their surroundings. In consequence, the country rock will receive heat and its temperature and/or melt fraction will rise. Repeated juxtaposition of hot melts with country rock is one mechanism for generating a substantial region of partial melt within the lower crust. A common misconception among modellers is that oceanic crustal material has a single uniform composition and therefore that its melting behaviour does not vary. It is important to note, however, that compositional variation in the crust, the result of magmatic differentiation, has important implications for the interpretation of geophysical data and its linkage to thermal models [36]. The development of mushy zones is also controlled by the melting interval of the country rock material.

If the nodules of cumulate material carried by Borgarhraun are representative of its country rock, then we can use them to explore the effect of the intrusion and cooling of hot mantle melts on the development of mush in the country rock.

A crystallization model, performed using the MELTS software [56,57], was used to investigate this problem. The purpose of this model was to generate a simple, self-consistent examination of the behaviour of cumulate wall-rock when intruded by a liquid with the same composition and temperature as its parent. First, a putative parental melt for the Borgarhraun tephra glasses was obtained by addition of equilibrium olivine. This parental melt was required to be in equilibrium with Fo<sub>90</sub> olivine. Then, the parental melt was cooled at a model pressure of 5 kbar until about 20% crystallization had taken place (figure 5). This range of fractional crystallization was sufficient to generate most of the range of olivine compositions observed in macrocryst cores in Borgarhraun, as well as providing olivine, clinopyroxene and plagioclase in the crystallization assemblage, matching the observed macrocryst mode. The liquid composition also lies within the field of observed high MgO basalts from Theistareykir [2].

The model olivine, clinopyroxene and plagioclase material generated by this crystallization interval was then converted into a mean cumulate composition, which has a composition similar to that of the mean observed cumulate clots in the Borgarhraun samples: about half ultramafic cumulates and half primitive cumulate gabbros [54]. The melting behaviour of this cumulate was then investigated using MELTS, so that a self-consistent relationship between the crystallizing

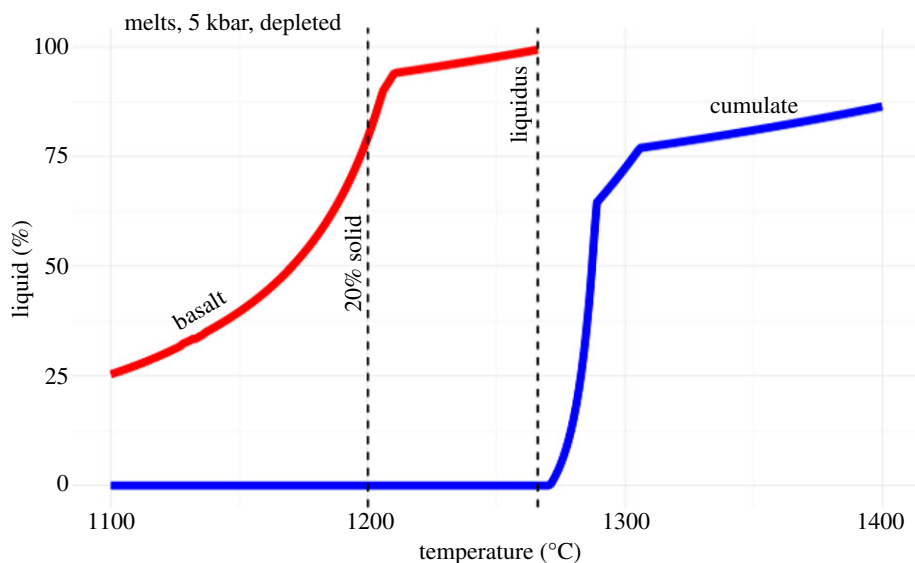


**Figure 5.** Results of MELTS calculations based roughly on the behaviour of expected Borgarhraun parental melt. The red curve (basalt) shows the melt fraction against temperature relationship for this melt during fractional crystallization. The blue curve (cumulate) shows the melting behaviour of a composition that corresponds to that of the solids generated during the first 20% of crystallization of the parental melt. This composition is solid at the liquidus temperature of the incoming primary melt. (Online version in colour.)

melt and the cumulate wall-rock could be obtained. The crucial point from figure 5 is that at the liquidus temperature of the initial melt, the cumulate composition is completely solid.

If the interstitial melt in the mush at the margins of the chamber can maintain chemical exchange with the primitive liquid in the interior, and the interstitial/oikocryst phases have compositions in equilibrium with that liquid rather than an evolved and isolated mush liquid, then it is possible to generate cumulate crust with a solidus temperature that is higher than the liquidus temperature of the intruded melt. This arrangement is consistent with a model where sills with high melt fractions sit in a country rock of hot, but solid, cumulate material. Pervasive mush is not formed in this case. The generation of widespread mush is hindered by effective chemical exchange between mush liquids and hot melts in the open chamber. The handful of observations of cumulate nodule compositions that are available from Borgarhraun [54,55] indicate cumulate formation Iceland appears to involve an effective chemical exchange, or, at least, the generation of primitive oikocrysts. Whole-rock and mineral compositions from near-Moho cumulates exposed in Oman also indicate that melt was effectively extracted, leaving behind cumulate rocks with compositions in equilibrium with primitive liquids [22,26–28]. Observations of oceanic cumulate rocks exposed on the sea-floor at Hess Deep are consistent with these observations from Oman and Iceland [58] and mafic plutonic rocks from the Pito Deep have been shown to contain trapped-melt fractions of less than 5% [59].

These observations and simple model results are consistent with a distribution of melt in the lower oceanic crust that is characterized by large alternations in melt fraction over lengthscales of metres, by open sills with thin mushy margins embedded in hot, but subsolidus, cumulates (figure 3*a*). This model hangs upon the generation of primitive cumulate rocks with very small trapped melt fractions: a crucial question for future study is to understand the process by which porosity is occluded in lower-crustal mushes.

## 6. Concurrent mixing and cooling: a constraint on sill thickness?

In the previous section, it was argued that the distribution of melt in the oceanic lower crust may be dominated by the presence of liquid sills encased in hot cumulate rock. The next question to

address is that of the characteristic thickness of such sills. The fact that individual melt bodies are difficult to image with geophysical approaches places an upper bound on their size on the scale of 100s of metres. Petrological and geological observations from ophiolites indicate that the melt layer thickness may be substantially smaller, perhaps as little as a metre. The vertical evolution of mineral compositions on the sub-metre scale in near-Moho cumulate gabbros from both Troodos [60] and Oman [26] have been used to support this finding. It is likely that these metre-scale estimates are minima because near-Moho bodies in ophiolites may have undergone some flattening after formation of the layering [26]. Nevertheless, the ratio of preserved cumulate layer thickness to original liquid thickness is likely to be preserved and [26] estimated that 5–20% crystallization took place in near-Moho melt lenses. This corresponds to a temperature drop of  $<20^{\circ}\text{C}$  for crystallization of basalt to generate cumulate gabbro.

Observational tests of these models of metre-scale melt-rich sills have been challenging to identify. However, detailed examination of the composition of melt inclusions, their olivine hosts and the carrier liquid in primitive basalts may provide a novel constraint on this problem. It is well known that melt inclusions trapped in forsteritic olivines from single samples preserve compositional heterogeneity that originates in the mantle [50]. This compositional variability is best understood using trace element ratios (such as La/Yb) or isotope ratios (e.g.  $^{207}\text{Pb}/^{206}\text{Pb}$ ) which are not strongly influenced by crustal processes (other than melt mixing). Ideally, these geochemical quantities can be used as passive tracers of the melt mixing process. The observations from a number of settings including Iceland, mid-ocean ridges and oceanic islands also indicate that as the forsterite content of the host olivine drops, the diversity of the melt inclusions in these trace element ratios also drops [43,61,62]. This observation can be accounted for by a model where concurrent mixing and crystallization of melts takes place in the magma storage zones (figure 4). In the following paragraphs, it is demonstrated that these observations may provide a novel constraint on the thickness of the melt layer in lower-crustal sills.

### (a) Petrological modelling

Quantitative models of magmatic processes require the evolution of the physical properties of the magma and its phases to be understood as a function of temperature. In order to determine the physical characteristics of the convecting melt, the method of [63] was used to calculate the viscosity and [64] the density. The melt temperatures and compositions were obtained by running a starting composition of primitive Icelandic glass from Borgarhraun through the PETROLOG software [65]. In order to generate a suitable primary melt for the calculations, olivine was added to the glass composition until the liquid was in equilibrium with  $\text{Fo}_{90}$  olivines. Then, the crystallization of this liquid at 5 kbar was modelled using PETROLOG.

### (b) Cooling and mixing time scales

The observations in figure 4 show that destruction of compositional variation of passive tracers (such as incompatible trace element ratios) in the melt is coupled to cooling of the melt as recorded in the composition of the crystallizing olivine. Melt mixing and cooling are concurrent.

If melt mixing were to proceed more rapidly than cooling, then heterogeneity in the passive tracer would either be entirely absent or limited to inclusions hosted in olivines with the very highest forsterite content on figure 4a. By contrast, if mixing is slower than cooling, then diversity in the compositional tracer should be preserved across the range of olivine compositions: figure 4a would show a broad band in variability in melt inclusion chemistry across the range of olivine compositions rather than the clear narrowing that is observed at low forsterite content.

The properties plotted on figure 4 are directly derived from the data and do not involve assumptions relating to a physical model. The time scale of the mixing and cooling processes cannot be directly estimated from these properties, but an examination of the relative rates of mixing and cooling may provide observational constraints on simple models of fluid convection within a sill. The fact that a record of concurrent mixing and cooling is preserved in the melt

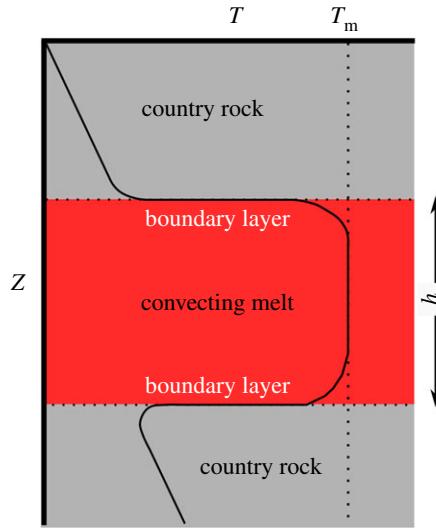


**Figure 6.** Model set-up for calculations relating to convection, cooling and mixing in a melt layer. (Online version in colour.)

inclusion observations indicates that the time scales of mixing and cooling must be similar. As will be demonstrated below, this equivalence of time scales provides a means of estimating sill thickness.

The time scale of conductive cooling,  $\tau_c$ , of the interior of a sill of thickness,  $h$ , (e.g. figure 6) is given by

$$\tau_c = \frac{h^2}{\kappa}, \quad (6.1)$$

where  $\kappa$  is the thermal diffusion coefficient. However, given the relatively low viscosity of hot basaltic melts and the availability of substantial buoyancy contrasts in the system, it is highly likely that vigorous convection will occur in basaltic magma bodies. This problem was examined by [66,67] who carried out a series of tank experiments involving fluids with highly temperature-dependent viscosity. They found that the temperature difference that drives convection,  $\Delta T_v$ , is linked to the temperature dependence of the fluid viscosity. The Rayleigh number of the chamber can then be approximated by

$$Ra_v = \frac{g\rho\alpha\Delta T_v h^3}{\kappa\mu} \quad (6.2)$$

with  $g$  being gravitational acceleration,  $\mu$  the temperature-dependent kinematic viscosity,  $\rho$  density,  $\alpha$  the thermal expansion coefficient and

$$\Delta T_v = \frac{\mu}{d\mu/dT}. \quad (6.3)$$

Following the expressions of [66–68], the characteristic cooling time scale in this case is given by

$$\tau_{vv} = 6.38\tau_c Ra_v^{-1/3}. \quad (6.4)$$

This approximation was developed to describe experiments where the upper boundary of the layer was held at a fixed temperature. However, when basalt is emplaced into country rock, the temperature of the roof rocks rises rapidly. In this case, the cooling of the chamber is controlled by the conductive flux of heat through the roof. The background heat flux,  $Q_c$ , imposed by a fixed

geothermal gradient at the time of intrusion,  $(dT/dz)_i$ , provides the minimum rate of heat loss from the chamber.

$$Q_c = k \left( \frac{dT}{dz} \right)_i \quad (6.5)$$

where  $k$  is the conductivity. The temperature difference driving the convection in the chamber can then be approximated by

$$\Delta T_c = \left( \frac{Q_c}{-0.47k_m} \right)^{3/4} \left( \frac{\kappa v}{\alpha g} \right)^{1/4} \quad (6.6)$$

and the corresponding Rayleigh number and cooling time are

$$Ra_{vc} = \frac{g \rho \alpha \Delta T_c h^3}{\kappa \mu} \quad (6.7)$$

and

$$\tau_{vc} = 6.38 \tau_c Ra_{vc}^{-1/3}. \quad (6.8)$$

This slow cooling by conduction through the roof rocks dictates that  $\tau_{vc}$  is an upper limit on the cooling time by convection in the chamber, while  $\tau_{vv}$  is a lower limit when cooling is rapid.

The time scale of mixing of passive chemical tracers in fluids convecting at high Rayleigh number has been studied by [69] and applied to magmatic systems by [70]. These authors expressed the mixing time as

$$\tau_h = \frac{1}{2\dot{\epsilon}} \log \left( \frac{\dot{\epsilon} h^2}{D} \right) \quad (6.9)$$

where  $D$  is the diffusion coefficient of the chemical tracer of interest and the strain rate is given as

$$\dot{\epsilon} = 0.023 \frac{\kappa}{h^2} Ra^{0.685}. \quad (6.10)$$

This equation allows the mixing time of passive tracers to be estimated for convection that is controlled by  $\Delta T_v$ , when  $Ra = Ra_{vv}$ , or convection that is driven by conductive cooling through the country rocks, when  $Ra = Ra_{vc}$ .

The equations (6.4), (6.8) and (6.9) can be used to estimate the time scales of mixing and cooling of basaltic chambers of different thicknesses, as shown on figure 7. The observational constraints presented in figure 4 indicate that the time scales of convective cooling,  $\tau_v$ , and mixing,  $\tau_h$ , are approximately equal. Inspection of figure 7 shows that  $\tau_v \sim \tau_m$  only when the basaltic chamber has a thickness of  $<5$  m. For thickness of  $>10$  m the cooling time scale becomes a factor of 10 or more longer than the mixing time.

The calculations presented in figure 7 were carried out for melt temperatures,  $T_m = 1200^\circ\text{C}$ ,  $T_b = 1150^\circ\text{C}$  and  $dT/dz = 0.38^\circ\text{C m}^{-1}$ . This magmatic temperature provides a viscosity estimate of  $\sim 3$  Pa s. For comparison, the range of crystallization temperatures estimated for the Borgarhraun olivines spans from  $1240$  to  $1350^\circ\text{C}$  [51,54]. If a higher  $T_m$  of  $1300^\circ\text{C}$  is used then the calculated viscosity is even lower, resulting in a sill thicknesses of about 2 m as the maximum where the time scales are equivalent.

## 7. Sill thickness, mush thickness and time scales

The simple analysis presented above indicates that convection in a sill with a convecting melt layer thickness of less than about 10 m can account for the observed geochemical evidence for concurrent mixing and crystallization in primitive Icelandic basalts. The crystallization interval associated with the range of forsterite contents observed in olivines from Borgarhraun is approximately 20% and if the mush porosity is 50% then we might expect a mush layer of  $\sim 4$  m thickness to form at the base of a 10 m thick sill. The simple convection calculations presented above provide a cooling time scale of  $\sim 10^6$  s, on the order of a month. This calculation implies that heat loss, magmatic cooling and crystallization can take place relatively rapidly.

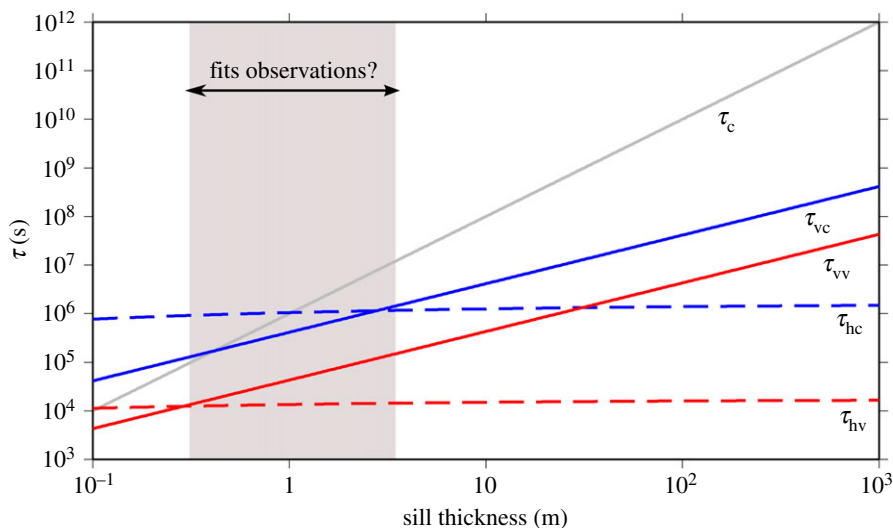


**Figure 7.** Characteristic time scales for cooling and mixing in a melt layer. The grey line is the conductive cooling time scale ( $\tau_c$ ). The blue solid line is the convective cooling time scale in the case where heat loss from the sill is controlled by the thermal gradient in the country rock ( $\tau_{vc}$ ). The red solid line is the convective cooling time scale for when the heat loss is controlled by the temperature-dependence of the viscosity of the melt ( $\tau_{vv}$ ). The dashed lines show the chemical homogenization time scales associated with these two convective cooling time scales. The grey shaded box shows the range of sill thicknesses that approximately match the observations. (Online version in colour.)

It has previously been suggested that the relationship between the distribution of olivine macrocryst core compositions and carrier liquid compositions in Borgarhraun and other Icelandic basalts reflects partial diffusive re-equilibration of Mg-Fe through the mush liquid [49]. These authors found that the distribution of olivine compositions observed in Borgarhraun can be generated in a  $\sim 5$  m thick mush pile after about  $3 \times 10^{10}$  s (about 1000 years). Some previous studies of the likely duration of basalt storage in the Icelandic crust are consistent with this time scale, but are poorly constrained [71,72]. Intriguingly, more detailed storage time scales have recently been obtained by the modelling of diffusion profiles in spinel inclusions from Borgarhraun, and indicate that crystals may be stored for about 1000 years in mushes prior to eruption [73].

## 8. Synthesis: evolution of a lower crustal sill

The observations from Borgarhraun can be combined with the results of simple physical reasoning to suggest a model of magmatic processes in the lower crust. This sequence of events is depicted in figure 8 and shows a scenario that may occur in the lowermost crust of the trans-crustal model shown in figure 1.

First, it is assumed that diverse mantle melts are fed rapidly to a sill. This chemical diversity, which is clearest in trace element ratios and isotope compositions, is depicted as varying shades of blue on figure 8 [43]. Estimates of Borgarhraun olivine crystallization temperatures [51,54,74] indicate that the melt has an injection temperature,  $T_m$  of over  $1300^\circ\text{C}$ . The country rock temperature is set at a temperature that is close to that of the liquidus of the erupted Borgarhraun melt [53,54] at  $T_b \sim 1230^\circ\text{C}$ . The results shown on figure 5 indicate that cumulate country rock can be solid at this temperature.

The analysis from the previous section (figure 7) indicates that the sill may have a vertical thickness of about about 10 m. The lateral extent of this body is not well constrained. If it is assumed that the supply of mantle melt to the sill was very rapid and that the entire volume

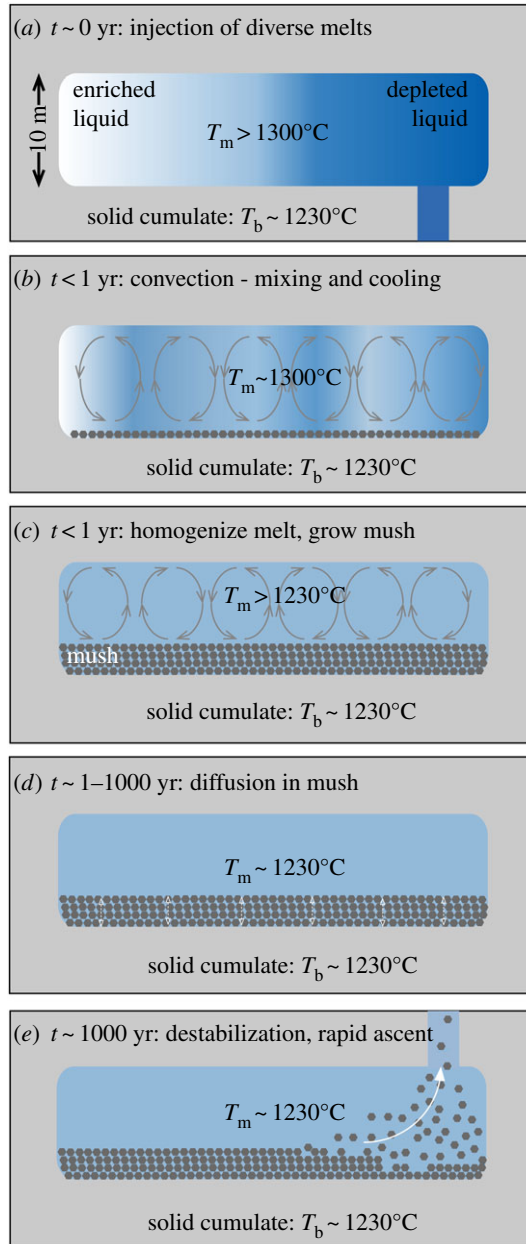


**Figure 8.** Evolution of a melt layer within the lower crust of an active magmatic system. See text for details. (Online version in colour.)

of erupted Borgarhraun lava,  $0.35 \text{ km}^3$  [51] was stored in a single sill, then the lateral extent of the sill would be  $35 \text{ km}^2$ . This area is similar to that of the Borgarhraun flow on the surface, equivalent to a disk with a radius of  $\sim 3 \text{ km}$ . The lateral extent of lower crustal melt sills imaged by reflection seismic data close to the East Pacific Rise is  $\sim 4 \text{ km}$  [75].

The large thermal gradients and low viscosities of the melts permit vigorous convection to take place (figure 8*b*). This convection is linked to rapid heat loss from the sill, and also to stirring of the heterogeneous mantle melts. The characteristic cooling and mixing time scales presented in figure 7 are short, and it is likely in this case that trace element homogenization of the melt will

occur in under a year. Cooling and crystallization are concurrent with this mixing, and fractional crystallization models from figure 5 and [51] indicate that about 20% crystallization can occur as the injected primary melt cools from the initial  $T_m$  towards  $T_b$ . The dense primitive crystals will settle rapidly to the base of the sill and form a mushy layer. If the initial porosity of this olivine-rich layer is close to 50%, then the mush thickness at the chamber base may be  $\sim 4$  m (figure 8c).

When the temperature difference between the melt and the country rock has dropped substantially, convection may weaken or halt (figure 8d). When the temperature variations are small, compositional variations play an increasingly important role in controlling the melt fraction. The basaltic liquid in the sill remains molten while the cumulate wall-rock is solid (figure 5). The distinctive distribution of olivine core compositions in Borgarhraun and other Icelandic eruptions has been interpreted as evidence for mush storage for  $\sim 1000$  years [49]. Diffusive exchange of Mg-Fe through the liquid and crystals of the mush pile may account for the olivine distributions. Recent diffusion chronometry results also indicate that spinel inclusions in crystalline nodules in Borgarhraun have been stored for  $\sim 1000$  years after their inclusion in a crystal framework [73].

After about a thousand years, a trigger event causes rupture of the sill, disaggregation of the mush pile and then rapid transfer of the magma towards the surface (figure 8e). Recent diffusion chronometry results constrain the transport time to be shorter than  $\sim 4$  days [53].

Diverse petrological observations from Icelandic basalts, and Borgarhraun in particular, indicate that melt is stored in sills of decimetric height within the lower crust. This view is consistent with the model of [26] for the accretion of material in the lower oceanic crust, which was based on observations from ophiolite sequences. The model of crustal accretion dominated by storage in small sills may have some general applicability to magmatic systems.

## 9. Conclusion

There is strong evidence from geophysics, geology and petrology to support a model of *trans-crustal* magmatism in the key magmatic settings on Earth. Iceland provides an excellent opportunity to develop and test models of magmatic processes and crustal accretion at spreading ridges more broadly. Petrological observations, modelled using a number of barometric methods, indicate that magma is stored and crystallizes in several tiers of magmatic bodies under Iceland, with the deepest of these being close to the Moho ( $>20$  km depth) and the shallowest at  $\sim 5$  km.

The barometric results also indicate that Icelandic magma can be fed directly from close to the Moho to the surface without being trapped and equilibrating at shallower levels. This rapid transport of melt from depth occurs even in the active rift zones of Iceland, where magma supply rates are high. Furthermore, the compositional relationship between melts, macrocrysts and melt-inclusions indicates that there is little petrological evidence of interaction between magma batches and the crust in the transit path between deep storage and eruption. Eruptions that are close in time and space have plumbing systems that are remarkably distinct. These observations indicate that the crust of several of Iceland's active rift zones (the NVZ, WVZ and Reykjanes Peninsula) is not composed of an extensive, pervasive mush.

Geophysical and petrological results from Iceland are consistent with a *stacked sills* mode of crustal accretion, a model that was developed in response to observations from active mid-ocean ridges and ophiolite complexes. In these models, thin and transient mushes may form at the margins of thin melt sills, meaning that many rising magmas carry evidence of interaction with mush and all solid cumulate rocks have progressed through a mushy stage. The melt sills are encased in a hot, but subsolidus country rock. In order to generate suitable cumulate country rock it is vital that porosity in mushes is occluded by the crystallization of primitive phases.

Geochemical evidence from Icelandic melt inclusion suites indicates that mixing and cooling of melts are concurrent in crustal magma storage zones. Convection is likely to couple these processes together and the fact that evidence for both mixing and cooling is preserved indicates



that the timescales of these processes are similar. Simple fluid dynamical reasoning can be used to show that this equivalence of time scales is expected from mixing in basaltic sills that are less than about 10 m in height. These sill thicknesses are very similar to those envisioned for oceanic crustal accretion at spreading ridges on the basis of observations at ophiolites.

**Data accessibility.** This article does not contain any additional data.

**Competing interests.** We declare we have no competing interests.

**Funding.** The conceptual basis of this project was developed during a Natural Environment Research Council fellowship held by JM: NER/I/S/2002/00609.

**Acknowledgements.** Thanks to John Rudge, Jerome Neufeld, Andy Woods and Christian Huber for discussing the model of cooling and mixing. Marian Holness provided useful advice about mushes and porosity evolution as preserved in plutonic rocks. Euan Mutch kindly shared his findings based on diffusion chronometry. The author would like to also thank two anonymous reviewers for providing detailed comments that significantly improved the clarity of the manuscript and the editors of this volume.

## References

1. Cashman KV, Sparks RSJ, Blundy JD. 2017 Vertically extensive and unstable magmatic systems: a unified view of igneous processes. *Science* **355**, eaag3055. (doi:10.1126/science.aag3055)
2. MacLennan J, McKenzie D, Gronvold K, Slater L. 2001 Crustal accretion under northern Iceland. *Earth Planet. Sci. Lett.* **191**, 295–310. (doi:10.1016/s0012-821x(01)00420-4)
3. MacLennan J. 2008 The supply of heat to mid-ocean ridges by crystallization and cooling of mantle melts. *AGU Monograph* **178**, 45–73. (doi:10.1029/178GM04)
4. Kelley DF, Barton M. 2006 Pressures of crystallization of Icelandic magmas. *J. Petrol.* **49**, 465–492. (doi:10.1093/petrology/egm089)
5. Thordarson T, Larsen G. 2007 Volcanism in Iceland in historical time: Volcano types, eruption styles and eruptive history. *J. Geodyn.* **43**, 118–152. (doi:10.1016/j.jog.2006.09.005)
6. Johannesson H, Sæmundsson K. 1998 *Geological map of Iceland*. Reykjavik, Iceland: Icelandic Institute of Natural History and Iceland Geodetic Survey
7. Jenkins J, MacLennan J, Green RG, Cottaar S, Deuss AF, White RS. 2018 Crustal formation on a spreading ridge above a mantle plume: receiver function imaging of the Icelandic crust. *J. Geophys. Res.* **123**, 5190–5208. (doi:10.1029/2017jb015121)
8. Holness M, Nielsen TFD, Tegner C. 2017 The Skaergaard intrusion of East Greenland: paradigms, problems and new perspectives. *Elements* **13**, 391–396. (doi:10.2138/gselements.13.6.391)
9. Grove TL, Kinzler RJ, Bryan WB. 1992 Fractionation of mid-ocean Ridge Basalt (MORB). *AGU Monograph* **71**, 281–310. (doi:10.1029/GM071p0281)
10. Yang H-J, Kinzler RJ, Grove TL. 1996 Experiments and models of anhydrous, basaltic, olivine-plagioclase-augite saturated melts from 0.001 to 10 kbar. *Contrib. Mineral. Petrol.* **124**, 1–18. (doi:10.1007/s004100050169)
11. Herzberg C. 2004 Partial crystallization of mid-ocean ridge basalts in the crust and mantle. *J. Petrol.* **45**, 2389–2405. (doi:10.1093/petrology/egh040)
12. Cannat C, Cann J, MacLennan J. 2004 Some hard-rock constraints on the supply of heat to mid-ocean ridges. *AGU Monograph* **148**, 20040101. (doi:10.1029/148GM05)
13. Putirka K, Johnson M, Kinzler RJ, Longhi J, Walker D. 1996 Thermobarometry of mafic igneous rocks based on clinopyroxene-liquid equilibria, 0–30 kbar. *Contrib. Mineral. Petrol.* **123**, 92–108. (doi:10.1007/s004100050145)
14. Neave DA, Putirka KD. 2017 A new clinopyroxene-liquid barometer, and implications for magma storage pressures under Icelandic rift zones. *Am. Mineral.* **102**, 777–794. (doi:10.2138/am-2017-5968)
15. Moore A, Coogan LA, Costa F, Perfit MR. 2014 Primitive melt replenishment and crystal-mush disaggregation in the weeks preceding the 2005–2006 eruption at 9°50'N, EPR. *Earth Planet. Sci. Lett.* **403**, 15–26. (doi:10.1016/j.epsl.2014.06.015)
16. Hartley ME, Morgan DJ, MacLennan J, Edmonds M, Thordarson T. 2016 Tracking timescales of short-term precursors to large basaltic fissure eruptions through Fe–Mg diffusion in olivine. *Earth Planet. Sci. Lett.* **439**, 58–70. (doi:10.1016/j.epsl.2016.01.018)

17. Pankhurst MJ, Morgan DJ, Thordarson T, Loughlin SC. 2018 Magmatic crystal records in time, space, and process, causatively linked with volcanic unrest. *Earth Planet. Sci. Lett.* **493**, 231–241. (doi:10.1016/j.epsl.2018.04.025)
18. Hansen H, Grönvold K. 2000 Plagioclase ultraphyric basalts in Iceland: the mush of the rift. *J. Volcanol. Geotherm. Res.* **98**, 1–32. (doi:10.1016/s0377-0273(99)00189-4)
19. Holness M, Anderson AT, Martin VM, Maclennan J, Passmore E, Schwindinger K. 2007 Textures in partially solidified crystalline nodules: a window into the pore structure of slowly cooled mafic intrusions. *J. Petrol.* **48**, 1243–1264. (doi:10.1093/petrology/egm016)
20. Keiding JK, Sigmarsson O. 2012 Geothermobarometry of the 2010 Eyjafjallajökull eruption: new constraints on Icelandic magma plumbing systems. *J. Geophys. Res.* **117**, B00C09. (doi:10.1029/2011jb008829)
21. Hartley ME, Bali E, Maclennan J, Neave DA, Halldórsson SA. 2018 Melt inclusion constraints on petrogenesis of the 2014–2015 Holuhraun eruption, Iceland. *Contrib Mineral Petrol* **173**, 10. (doi:10.1007/s00410-017-1435-0)
22. Kelemen PB, Koga K, Shimizu N. 1997 Geochemistry of gabbro sills in the crust/mantle transition zone of the Oman ophiolite: implications for the origin of the oceanic lower crust. *Earth Planet. Sci. Lett.* **146**, 475–488. (doi:10.1016/S0012-821X(96)00235-X)
23. Sinton JM, Detrick RS. 1992 Mid-ocean ridge magma chambers. *J. Geophys. Res.* **97**, 197–216. (doi:10.1029/91jb02508)
24. Perfit MR, Fornari DJ, Smith MC, Bender JF, Langmuir CH, Haymon RM. 1994 Small-scale spatial and temporal variations in mid-ocean ridge crest magmatic processes. *Geology* **22**, 375–379. (doi:10.1130/0091-7613(1994)022<0375:sssatv>2.3.co;2)
25. Solano JMS, Jackson MD, Sparks RSJ, Blundy J. 2014 Evolution of major and trace element composition during melt migration through crystalline mush: Implications for chemical differentiation in the crust. *Am. J. Sci.* **314**, 895–939. (doi:10.2475/05.2014.01)
26. Korenaga J, Kelemen PB. 1997 The origin of gabbro sills in the Moho transition zone of the Oman ophiolite: implications for magma transport in the oceanic lower crust. *J. Geophys. Res.* **102**, 27 729–27 749. (doi:10.1029/97jb02604)
27. Korenaga J, Kelemen PB. 1998 Melt migration through the oceanic lower crust: a constraint from melt percolation modeling with finite solid diffusion. *Earth Planet. Sci. Lett.* **156**, 1–11. (doi:10.1016/S0012-821X(98)00004-1)
28. Koga K, Kelemen PB, Shimizu N. 2001 Petrogenesis of the crust-mantle transition zone (MTZ) and the origin of lower crustal wehrlite in the Oman Ophiolite. *Geochem. Geophys. Geosyst.* **2**, 2000GC000132. (doi:10.1029/2000gc000132)
29. Greenfield T, White RS, Roecker S. 2016 The magmatic plumbing system of the Askja central volcano, Iceland, as imaged by seismic tomography. *J. Geophys. Res.* **121**, 7211–7229. (doi:10.1002/2016jb013163)
30. Detrick RS, Buhl P, Vera E, Mutter J, Orcutt J, Madsen J, Brocher T. 1987 Multichannel seismic imaging of a crustal magma chamber along the East Pacific Rise between 9°N and 13°N. *Nature* **326**, 35–41. (doi:10.1038/326035a0)
31. Singh SC, Kent GM, Collier JS, Harding AJ, Orcutt JA. 1998 Melt to mush variations in crustal magma properties along the ridge crest at the southern East Pacific Rise. *Nature* **394**, 874–878. (doi:10.1038/29740)
32. Canales JP, Nedimovic MR, Kent GM, Carbotte SM, Detrick RS. 2009 Seismic reflection images of a near-axis melt sill within the lower crust at the Juan de Fuca ridge. *Nature* **460**, 89–93. (doi:10.1038/nature08095)
33. Carbotte SM, Marjanovic M, Carton H, Mutter JC, Canales JP, Nedimovic MR, Han S, Perfit MR. 2013 Fine-scale segmentation of the crustal reservoir beneath the East Pacific Rise. *Nat. Geosci.* **6**, 866–870. (doi:10.1038/ngeo1933)
34. Sleep NH. 1975 Formation of oceanic crust: some thermal constraints. *J. Geophys. Res.* **80**, 4037–4042. (doi:10.1029/jb080i029p04037)
35. Henstock TJ, Woods AW, White RS. 1993 The accretion of oceanic crust by episodic sill intrusion. *J. Geophys. Res.* **98**, 4143–4161. (doi:10.1029/92jb02661)
36. Maclennan J, Hulme T, Singh SC. 2004 Thermal models of oceanic crustal accretion: Linking geophysical, geological and petrological observations. *Geochem. Geophys. Geosyst.* **5**, Q02F25. (doi:10.1029/2003GC000605)

37. Hasenclever J, Theissen-Krah S, Rupke L, Morgan JP, Iyer K, Petersen S, Devey CW. 2014 Hybrid shallow on-axis and deep off-axis hydrothermal circulation at fast-spreading ridges. *Nature* **508**, 508–512. (doi:10.1038/nature13174)
38. Bryan WB, Moore JG. 1977 Compositional variations of young basalts in the Mid-Atlantic Ridge rift valley near lat 36°49'N. *Geol. Soc. Am. Bull.* **88**, 556. (doi:10.1130/0016-7606(1977)88<556:cvoybi>2.0.co;2)
39. Quick JE, Denlinger RP. 1993 Ductile deformation and the origin of layered gabbro in ophiolites. *J. Geophys. Res.* **98**, 14 015–14 027. (doi:10.1029/93jb00698)
40. Chen YJ, Morgan JP. 1993 The genesis of oceanic crust: magma injection, hydrothermal circulation and crustal flow. *J. Geophys. Res.* **98**, 6283–6297. (doi:10.1029/92jb02650)
41. Sun C, Lissenberg CJ. 2018 Formation of fast-spreading lower oceanic crust as revealed by a new Mg-REE coupled geospeedometer. *Earth Planet. Sci. Lett.* **487**, 165–178. (doi:10.1016/j.epsl.2018.01.032)
42. Lissenberg C, MacLeod C. 2017 A reactive porous flow control on mid-ocean ridge magmatic evolution. *J. Petrol.* **57**, 2195–2220. (doi:10.1093/petrology/egw074)
43. MacLennan J. 2008 Concurrent mixing and cooling of melts under Iceland. *J. Petrol.* **49**, 1931–1953. (doi:10.1093/petrology/egn052)
44. Hartley ME, Thordarson T. 2013 The 1874–1876 volcano-tectonic episode at Askja, North Iceland: lateral flow revisited. *Geochem. Geophys. Geosyst.* **14**, 2286–2309. (doi:10.1002/ggge.20151)
45. Sinton J, Grönvold K, Sæmundsson K. 2005 Postglacial eruptive history of the Western Volcanic Zone, Iceland. *Geochem. Geophys. Geosyst.* **6**, Q12009. (doi:10.1029/2005gc001021)
46. Gee MAM, Thirlwall MF, Taylor RN, Lowry D, Murton BJ. 1998 Crustal processes: major controls on Reykjanes Peninsula Lava Chemistry, SW Iceland. *J. Petrol.* **39**, 819–839. (doi:10.1093/petrology/39.5.819)
47. Thordarson T, Hoskuldsson A. 2008 Postglacial volcanism in Iceland. *Jökull* **58**, 197–228.
48. Brandsdóttir B, Menke W, Einarsson P, White RS, Staples RK. 1997 Färoe-Iceland ridge experiment 2. Crustal structure of the Krafla central volcano. *J. Geophys. Res.* **102**, 7867–7886. (doi:10.1029/96jb03799)
49. Thomson AR, MacLennan J. 2012 The distribution of olivine compositions in Icelandic basalts and picrites. *J. Petrol.* **54**, 745–768. (doi:10.1093/petrology/egs083)
50. MacLennan J. 2008 Lead isotope variability in olivine-hosted melt inclusions from Iceland. *Geochim. Cosmochim. Acta* **72**, 4159–4176. (doi:10.1016/j.gca.2008.05.034)
51. MacLennan J, McKenzie D, Hilton F, Grönvold K, Shimizu N. 2003 Geochemical variability in a single flow from northern Iceland. *J. Geophys. Res.* **108**, ECV 4-1–ECV 4-21. (doi:10.1029/2000jb000142)
52. Neave DA, Passmore E, MacLennan J, Fitton G, Thordarson T. 2013 Crystal-melt relationships and the record of deep mixing and crystallisation in the AD 1783 Laki eruption, Iceland. *J. Petrol.* **54**, 1661–1690. (doi:10.1093/petrology/egt027)
53. Mutch EJJ, MacLennan J, Shorttle O, Edmonds M, Rudge J. Submitted. Rapid trans-crustal magma movement under Icelandic volcanoes. *Nat. Geosci.*
54. MacLennan J, McKenzie D, Grönvold K, Shimizu N, Eiler JM, Kitchen N. 2003 Melt mixing and crystallization under Theistareykir, northeast Iceland. *Geochem. Geophys. Geosyst.* **4**, 8624. (doi:10.1029/2003gc000558)
55. Winpenny B, MacLennan J. 2011 A partial record of mixing of mantle melts preserved in Icelandic phenocrysts. *J. Petrol.* **52**, 1791–1812. (doi:10.1093/petrology/egr031)
56. Ghiorso MS, Sack RO. 1995 Chemical mass transfer in magmatic processes IV. A revised and internally consistent thermodynamic model for the interpolation and extrapolation of liquid-solid equilibria in magmatic systems at elevated temperatures and pressures. *Contrib. Min. Petrol.* **119**, 197–212. (doi:10.1007/BF00307281)
57. Smith PM, Asimow PD. 2005 ADIABAT\_1PH: a new public front-end to the MELTS, pMELTS, and pHMELTS models. *Geochem. Geophys. Geosyst.* **6**, 1127. (doi:10.1029/2004gc000816)
58. Arai S, Takemoto Y. 2007 Mantle wehrlite from Hess Deep as a crystal cumulate from an ultra-depleted primary melt in East Pacific Rise. *Geophys. Res. Lett.* **34**, L08302. (doi:10.1029/2006gl029198)
59. Perk NW, Coogan LA, Karson JA, Klein EM, Hanna HD. 2007 Petrology and geochemistry of primitive lower oceanic crust from Pito Deep: implications for the accretion of the lower crust

- at the Southern East Pacific rise. *Contrib. Mineral. Petrol.* **154**, 575–590. (doi:10.1007/s00410-007-0210-z)
60. Browning P, Roberts S, Alabaster T. 1989 Fine-scale modal layering and cyclic units in ultramafic cumulates from the CY-4 Borehole, Troodos Ophiolite; evidence for an open system magma chamber. Geological Survey of Canada.
  61. Shorttle O, Rudge JF, Maclennan J, Rubin KH. 2016 A statistical description of concurrent mixing and crystallization during MORB differentiation: implications for trace element enrichment. *J. Petrol.* **57**, 2127–2162. (doi:10.1093/ptrology/egw056)
  62. Jennings ES, Gibson SA, Maclennan J, Heinonen JS. 2017 Deep mixing of mantle melts beneath continental flood basalt provinces: constraints from olivine-hosted melt inclusions in primitive magmas. *Geochim. Cosmochim. Acta* **196**, 36–57. (doi:10.1016/j.gca.2016.09.015)
  63. Giordano D, Russell JK, Dingwell DB. 2008 Viscosity of magmatic liquids: a model. *Earth Planet. Sci. Lett.* **271**, 123–134. (doi:10.1016/j.epsl.2008.03.038)
  64. Lange RL, Carmichael ISE. 1990 Thermodynamic properties of silicate liquids with emphasis on density, thermal expansion and compressibility. *Rev. Mineral. Geochem.* **24**, 25–64.
  65. Danyushevsky LV, Plechov P. 2011 Petrolog3: integrated software for modeling crystallization processes. *Geochem. Geophys. Geosyst.* **12**, Q07021. (doi:10.1029/2011GC003516)
  66. Davaille A, Jaupart C. 1993 Transient high-Rayleigh-number thermal convection with large viscosity variations. *J. Fluid Mech.* **253**, 141–166. (doi:10.1017/s0022112093001740)
  67. Davaille A, Jaupart C. 1994 Onset of thermal convection in fluids with temperature-dependent viscosity: application to the oceanic mantle. *J. Geophys. Res.* **99**, 19 853–19 866. (doi:10.1029/94jb01405)
  68. Jaupart C, Brandeis GL. 1986 The stagnant bottom layer of convecting magma chambers. *Earth Planet. Sci. Lett.* **80**, 183–199. (doi:10.1016/0012-821x(86)90032-4)
  69. Coltice N, Schmalzl J. 2006 Mixing times in the mantle of the early Earth derived from 2-D and 3-D numerical simulations of convection. *Geophys. Res. Lett.* **33**, L23304. (doi:10.1029/2006gl027707)
  70. Huber C, Bachmann O, Manga M. 2009 Homogenization processes in silicic magma chambers by stirring and mushification (latent heat). *Earth Planet. Sci. Lett.* **283**, 38–47. (doi:10.1016/j.epsl.2009.03.029)
  71. Maclennan J, Jull M, McKenzie D, Slater L, Gronvold K. 2002 The link between volcanism and deglaciation in Iceland. *Geochem. Geophys. Geosyst.* **3**, 1–25. (doi:10.1029/2001gc000282)
  72. Cooper K, Sims KWW, Eiler JM, Banerjee N. 2016 Timescales of storage and recycling of crystal mush at Krafla Volcano, Iceland. *Contrib. Mineral. Petrol.* **171**, 54. (doi:10.1007/s00410-016-1267-3)
  73. Mutch EJJ, Maclennan J, Holland TJB, Buisman I. Submitted. Millennial storage of near-Moho magma. *Nature*.
  74. Matthews S, Shorttle O, Maclennan J. 2016 The temperature of the Icelandic mantle from olivine-spinel aluminum exchange thermometry. *Geochem. Geophys. Geosyst.* **17**, 4725–4752. (doi:10.1002/2016GC006497)
  75. Canales JP, Carton H, Carbotte SM, Mutter JC, Nedimović MR, Xu M, Aghaei O, Marjanović M, Newman K. 2012 Network of off-axis melt bodies at the East Pacific Rise. *Nat. Geosci.* **5**, 279–283. (doi:10.1038/ngeo1377)